analytical chemistry

Article

pubs.acs.org/ac

Measurement of Protein Kinase B Activity in Single Primary Human Pancreatic Cancer Cells

Angela Proctor,[†] S. Gabriela Herrera-Loeza,[‡] Qunzhao Wang,[†] David S. Lawrence,[†,§] Jen Jen Yeh,[∥] and Nancy L. Allbritton*[,†,⊥]

[†]Department of Chemistry, University of North Carolina, Chapel Hill, North Carolina 27599, United States

[‡]Lineberger Comprehensive Cancer Center, University of North Carolina School of Medicine, Chapel Hill, North Carolina 27599, United States

[§]Division of Chemical Biology and Medicinal Chemistry, School of Pharmacy, University of North Carolina, Chapel Hill, North Carolina 27599, United States

[∥]Departments of Surgery and Pharmacology, University of North Carolina, Chapel Hill, North Carolina 27599, United States

[⊥]Department of Biomedical Engineering, University of North Carolina, Chapel Hill, North Carolina 27599, United States and North Carolina State University, Raleigh, North Carolina 27695, United States

Supporting Information

ABSTRACT: An optimized peptide substrate was used to measure protein kinase B (PKB) activity in single cells. The peptide substrate was introduced into single cells, and capillary electrophoresis was used to separate and quantify nonphosphorylated and phosphorylated peptide. The system was validated in three model pancreatic cancer cell lines before being applied to primary cells from human pancreatic adenocarcinomas propagated in nude mice. As measured by phosphorylation of peptide substrate, each tumor cell line exhibited statistically different median levels of PKB activity (65%, 21%, and 4% phosphorylation in PANC-1 (human pancreatic carcinoma), CFPAC-1 (human metastatic ductal pancreatic adenocarcinoma), and HPAF-II cells (human pancreatic adenocarcinoma), respectively) with CFPAC-1 cells demonstrating two populations of cells or bimodal behavior in PKB activation levels. The primary cells exhibited highly variable PKB activity at the single cell level, with some cells displaying little to no activity and others possessing very high levels of activity. This system also enabled simultaneous characterization of peptidase action in single cells by measuring the amount of cleaved peptide substrate in each cell. The tumor cell lines displayed degradation rates statistically similar to one another (0.02, 0.06, and 0.1 zmol pg^{-1} s^{-1}, for PANC-1, CFPAC-1, and HPAF-II cells, respectively) while the degradation rate in primary cells was 10-fold slower. The peptide cleavage sites also varied between tissue-cultured and primary cells, with 5- and 8-residue fragments formed in tumor cell lines and only the 8-residue fragment formed in primary cells. These results demonstrate the ability of chemical cytometry to identify important differences in enzymatic behavior between primary cells and tissue-cultured cell lines.

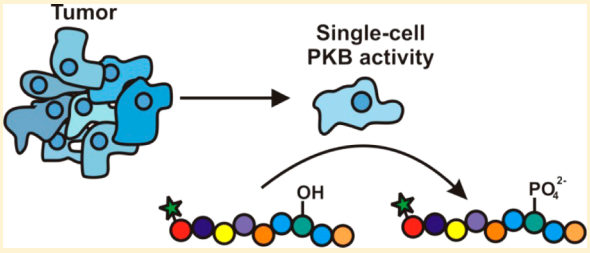

Pancreatic ductal adenocarcinoma (PDA) accounts for greater than 90% of all types of pancreatic cancer and is the fourth most common cause of cancer-related deaths in the United States.[1−4] PDA generally develops in adults over 50 years old adjacent to the pancreatic duct, often leading to blockage of the pancreatic or bile ducts. PDA tumors frequently invade deep into the pancreas and nearby organs and rapidly metastasize to the lymph nodes prior to diagnosis.[5,6] The American Cancer Society estimates that there will be approximately 45,220 new cases of PDA and 38,460 deaths from PDA in the United States in 2013.[5] Median survival for patients diagnosed early (Stage I) is approximately 2 years, but greater than 50% of individuals are not diagnosed until the late stages, when the median survival decreases to 4.5 months.[5] Treatment for patients with PDA includes surgical removal of the cancer (approximately 20% of patients) as well as radiation and chemotherapy, though these measures usually only relieve symptoms and may briefly extend survival. Only rarely does treatment yield a cure.[5]

Genetic alterations, including mutations, deletions, and amplifications, of up to 12 different signaling pathways and processes have been found in most pancreatic cancers, including PDA.[7] Among the pathways affected are those that control apoptosis, DNA damage control, and tumor invasion, all of which enable PDA tumors to survive and proliferate even in the presence of anticancer therapies.[8,9] Prominent among these altered pathways is the PI3-K (phosphoinositide 3-kinase) pathway, which regulates multiple cellular functions,

Received: February 13, 2014
Accepted: April 9, 2014
Published: April 9, 2014

   dx.doi.org/10.1021/ac500616q | *Anal. Chem.* 2014, 86, 4573−4580

including transcription, proliferation, stress response, and apoptosis.[10,11] Protein kinase B (PKB, also known as Akt) is a serine/threonine kinase in the PI3-K pathway whose activity has been implicated in providing cancer cells with antiapoptotic properties, even in the presence of multiple apoptotic stimuli.[8] This is particularly true in PDA, where the PI3-K/PKB pathway has been found to be constitutively active and appears to be an indicator of aggressiveness of the pancreatic cancer, with high levels of active PKB associated with decreased patient survival.[12−16] While 10% of analyzed pancreatic carcinomas show an amplification of AKT2 (one of 3 PKB genes), no other genetic alterations have been reported for PKB or PI3-K in pancreatic tumors, suggesting that alterations to the pathway are occurring by misregulation of mRNA, protein levels, or input from other pathways.[2,17] Thus, PKB gene copy number and protein levels often do not predict the level of PKB activity in a tumor. Consequently, a strategy to directly measure PKB activity in PDA tumors would be of high utility in understanding PKB signaling in PDA.

Currently, the most commonly utilized measurement of PKB in resected PDA tumors is Western blot analysis, in which the amount of active PKB is determined using antibodies directed against phosphorylated PKB.[2] However, this method reports the population-averaged level of PKB activity and yields no insight into tumor heterogeneity at the cellular level. It has long been known that tumors are highly heterogeneous, with differences arising from genetic, protein, and metabolic diversity.[18−20] By nature, bulk measurements cannot reveal these differences, whereas interrogation of single cells has the power to yield a wealth of information on single-cell dynamics. Immunohistochemistry (IHC) measurement of phosphorylated PKB has been used to assess PKB activity at the single-cell level.[2,12,14,15] Although IHC is valuable for determining subcellular localization of active PKB in PDA tumor cells, it is not quantitative. In contrast, chemical cytometry,[21] which utilizes sensitive analytical techniques to gather quantitative data from individual cells, provides a direct single-cell quantitative measurement of PKB activity.[22] The application of chemical cytometry for the analysis of PKB activity from individual PDA tumor cells should furnish a comprehensive assessment of PKB signaling heterogeneity within a tumor biopsy.

Patient-derived xenograft (PDX) tumors have enabled novel insights into human tumor cell biology as well as measurement of tumor-cell response to pharmacologic therapies. PDX tumors are formed by subcutaneously implanting a small fragment of primary tumor into an immunocompromised mouse.[23] PDX cells can then be passaged over time to form a renewable tissue resource. PDX models recapitulate the human tumor microenvironment and maintain both the gene-expression and genomic profiles as well as the morphology of the original human tumor.[23−27] Detailed IHC and allelotype analysis of PDA-derived xenografts have demonstrated that the degree of differentiation and nuclear polymorphisms in the original tumor sample are maintained immediately after establishment and following serial passage from one nude mouse to another.[28] PDX models are one of the most promising models to deliver personalized therapeutics for pancreatic cancer patients by permitting initial drug prescreening within the murine host.[25] Furthermore, PDX models provide an abundant and renewable source of primary PDA cells which can be utilized to identify the aberrant signaling pathways within single tumor cells.

In this work, capillary electrophoresis with laser-induced fluorescence detection (CE-LIF) has been employed to quantify PKB activity in single cells from tissue-cultured models of PDA as well as from PDX tumors. A PKB substrate was introduced into single cells, and the formation of phosphorylated product was quantified at varying times and substrate concentrations. For both model systems, the time-averaged rates of peptide phosphorylation and proteolysis within the single cells were measured at varying times and peptide concentrations. The impact of the inhibitor wortmannin, an irreversible inhibitor of PI3-K, was assessed on peptide phosphorylation and degradation to understand drug effects on both metabolic processes. Comparisons between single cells and among the primary PDX tumor cells and cultured cell lines revealed important differences in the cell-to-cell variability within cells from the same population as well as between cell types.

EXPERIMENTAL SECTION

Materials, Peptide Synthesis, and Statistical Analysis. Detailed information on materials, synthesis of peptides, and the statistical analyses utilized can be found in the Supporting Information.

Immortalized Cell Culture. PANC-1 (human pancreatic carcinoma), CFPAC-1 (human metastatic ductal pancreatic adenocarcinoma), HPAF-II (human pancreatic adenocarcinoma), and WI-38 (human lung tissue) cells were obtained from the American Type Culture Collection.[29−32] PANC-1 cells were cultured in Dulbecco's Modified Eagle Medium (DMEM) supplemented with 10% fetal bovine serum (FBS), penicillin (100 units mL^{-1}), and streptomycin (100 μg mL^{-1}). CFPAC-1 cells were grown in IMDM supplemented with 10% FBS, penicillin (100 units mL^{-1}), and streptomycin (100 μg mL^{-1}). HPAF-II and WI-38 cells were propagated in MEM supplemented with 10% FBS, penicillin (100 units mL^{-1}), and streptomycin (100 μg mL^{-1}). All cells were maintained in a humidified atmosphere of 37 °C in 5% CO_2 and passaged into fresh media every 2−3 days. Cells used for single-cell CE experiments were plated the day before the experiments onto custom chambers, prepared by using poly(dimethylsiloxane) (PDMS, Sylguard 184) to glue a silicon O-ring (McMaster-Carr) to a #1 glass coverslip (Fisher). A dilute cell suspension was added to 500 μL of the appropriate media in the chamber, and chambers were placed in the humidified incubator until use in the experiments.

Cell Preparation from Patient-Derived Xenografts. Pancreatic tumor tissue from deidentified patients were engrafted subcutaneously into the flanks of NSG/NOD (nonobese diabetic scid gamma/nonobese diabetic) mice, expanded, and passed over time. All animal experiments were carried out ethically under protocols approved by the University of North Carolina Institutional Animal Care and Use Committee.[27,33] Harvested tumors were immersed in phosphate buffered saline (PBS; 137 mM NaCl, 27 mM KCl, 10 mM Na_2HPO_4, 1.75 mM KH_2PO_4, pH 7.4) with penicillin (500 units mL^{-1}) and streptomycin (500 μg mL^{-1}) and dissected into small fragments. Tumors were disaggregated by incubating at 37 °C for 20−40 min in 40 mg mL^{-1} collagenase D and Dispase II. After incubation, the mixture was centrifuged at 1500g for 2 min prior to suspension in fresh media. The cell suspensions were immediately plated onto cell chambers and cultured in DMEM supplemented with 10% FBS, penicillin (100 units mL^{-1}), and streptomycin (100 μg mL^{-1}) and

dx.doi.org/10.1021/ac500616q | Anal. Chem. 2014, 86, 4573−4580

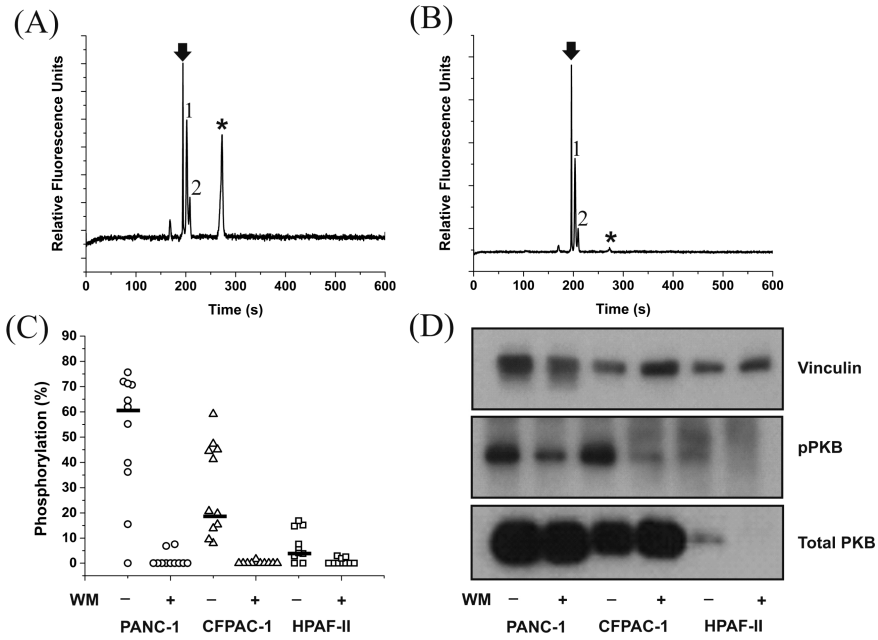

Figure 1. Representative electropherograms from single-cell analysis of PANC-1 tissue-cultured cells without (A) and with (B) treatment with wortmannin (WM). Peptide was incubated in cells for 5 min prior to analysis (A–C). The solid arrow indicates intact parent peptide, and the asterisk indicates phosphorylated peptide. Peaks labeled 1 and 2 correspond to the 8- and 5-residue fragment peptides, respectively. Single-cell CE (C) and Western blot (D) results of PKB activity assessment in tissue-cultured cells. The bars represent the median (C). Vinculin was used as a loading standard (D).

maintained in a humidified atmosphere at 37 °C in 5% CO_2. The chambers used for single-cell experiments were made of a thin film of polystyrene (146 ± 10 μm thick) prepared with 10% polystyrene in GBL and baked at 90 °C for 4 h and 120 °C for 20 h, as described previously.[34] PDMS was used to glue a silicon O-ring (McMaster-Carr) to the polystyrene thin film to create the chamber. Chambers were oxygen-plasma treated for 5 min and used either uncoated or coated with 0.1% gelatin. To enable surface attachment, cells were plated in the chambers 36 h prior to use.

Western Blot. PANC-1, CFPAC-1, and HPAF-II cell lysates were prepared on ice with RIPA buffer with protease and phosphatase inhibitors. Cells treated with wortmannin were incubated in 1 μM wortmanin for 10 min prior to lysis. Protein extracts were quantified for total protein with a Bradford Assay. The lysates were separated by sodium dodecyl sulfate-polyacrylamide gel electrophoresis (SDS-PAGE) prior to transfer to a PVDF membrane. Primary antibodies were antiphospho-PKB (Ser473) rabbit antibody; anti-PKB rabbit antibody directed against total PKB; and antivinculin mouse antibody directed against vinculin. Secondary antibodies were antirabbit or antimouse IgG conjugated to horseradish peroxidase (HRP). Samples were visualized using an electrochemiluniescent substrate for HRP.

Single-Cell CE. Chambers with cells were placed on the microscope stage and perfused with extracellular buffer [ECB; 135 mM NaCl, 5 mM KCl, 1 mM $MgCl_2$, 1 mM $CaCl_2$, and 10 mM *N*-2-hydroxyethylpiperazine-*N*′-2-ethanesulfonic acid (HEPES), pH 7.4, 37 °C] to remove culture media. To calculate cell volume, PDX tumor cells were modeled as spheres and tissue-cultured cells were modeled as rectangles with a height of 3 μm. Cell volume ranged from 1 to 15 pL, with 62% of the cells between 3 and 8 pL. Peptide VI-B was introduced into single cells by microinjection using finely pulled glass capillaries (FemtoJet Injectman NI 2, Eppendorf, Hauppauge, NY) and an injection pressure of 200 hPa for 0.5 s. A single cell was microinjected with peptide VI-B and incubated in ECB (37 °C) flowing at 3 mL min^{-1}.

Single-cell CE was performed using a custom-built CE system mounted on a microscope stage coupled to laser-induced fluorescence detection as described previously.[35,36] A detailed description of the custom-built system can be found in the Supporting Information. Fused silica capillaries [30 μm inner diameter, 360 μm outer diameter (Polymicro Technologies, Phoenix, AZ)] had a total length of 38 cm and an effective length of 21.5 cm. The electrophoretic buffer was 300 mM borate, pH 7.5, and a field strength of 260 V was applied for separations. Electrophoresis was initiated by application of a negative voltage to the outlet while the inlet was held at ground. For single cells, the capillary was positioned approximately 20 μm above the cell of interest prior to cell lysis. A focused pulse (5 ns) from an Nd:YAG laser created a cavitation bubble which mechanically lysed the cell. Simultaneously, −3 kV was applied to the capillary inlet while the outlet was held at ground so that the cell's contents were electrokinetically loaded into the capillary inlet. The capillary inlet was then transferred to an electrophoretic buffer reservoir and electrophoresis initiated.

To treat cells with the inhibitor wortmannin, media was removed from the cell chamber and replaced with 500 μL of 500 nM wortmannin in the appropriate cell media. The cells were incubated for 10 min in a 37 °C humidified incubator. Cells were then treated as described above. To estimate the amount of peptide in each cell, a known concentration of each peptide was hydrodynamically loaded into the capillary and electrophoresed, and the area under the resulting peak was calculated. Poiseuille's equation was utilized to estimate the amount of peptide loaded into the capillary.[37] Initial substrate concentration in each cell was determined by dividing the calculated number of moles microinjected into each cell by the estimated cell volume.

dx.doi.org/10.1021/ac500616q | *Anal. Chem.* 2014, 86, 4573–4580

Antibody Staining. All PDX tumor samples were stained with antihuman EpCAM antibody conjugated to AlexaFluor647 prior to single cell analysis. EpCAM-positive PANC-1 cells and EpCAM-negative WI-38 cells were used as controls for antibody staining. Cells in chambers were rinsed with ECB and incubated in a 1:40 solution of anti-EpCAM in ECB for 15 min in a humidified 37 °C incubator. Cells were rinsed with ECB prior to imaging (excitation = 620 ± 20 nm, emission = 690 ± 30 nm) using a CoolSnap HQ^2 CCD camera (Photometrics, Tucson, AZ). Only cells staining positive for EpCAM were microinjected with peptide and analyzed by CE.

RESULTS AND DISCUSSION

Characterization of Peptidase Activity in Single Tissue-Cultured Cells Derived from Pancreatic Adenocarcinomas. Three representative pancreatic cancer cell lines were selected on the basis of their variability in PKB activity. PANC-1 cells were derived from a 56-year old Caucasian male with pancreatic cancer;[31] CFPAC-1 cells were derived from the liver of a 26-year old Caucasian male with cystic fibrosis and pancreatic cancer;[30] and HPAF-II cells were obtained from a human pancreatic carcinoma isolated from the ascitic fluid of a 44-year old Caucasian male with primary pancreatic adenocarcinoma and metastases to the liver, diaphragm, and lymph nodes.[29] To assess the degradation of peptide-based reporters in these tumor lines, a previously validated, peptidase-resistant PKB substrate (peptide VI-B, *6FAM*-GRP-MeArg-AFTF-MeAla-NH_2)[22] was microinjected into single cells. After a 5 min incubation, the cell was lysed and the cellular contents separated by capillary electrophoresis. Peaks were identified as intact peptide, phosphorylated peptide, and fragment peptide based on comigration with standards. When peptide VI-B was incubated in PANC-1 (n = 11), CFPAC-1 (n = 11), or HPAF-II (n = 10) cells for 5 min, four peaks were present on the electropherograms, corresponding to intact peptide, phosphorylated peptide, and two fragment peptides (Figures 1A and S1, Supporting Information). The fragment peptides were identified as the 5- and 8-residue fragments of the parent peptide. The intact parent peptide accounted for 23 ± 10%, 39 ± 13%, and 45 ± 2% of total peptide in PANC-1, CFPAC-1, and HPAF-II cells, respectively. The abundances of the two fragment peptides were similar among the three cell lines, with PANC-1, CFPAC-1, and HPAF-II cells possessing 12 ± 3%, 9 ± 5%, and 10 ± 2% of the 5-residue fragment and 38 ± 10%, 36 ± 17%, and 41 ± 4% of the 8-residue fragment, respectively, after 5 min. These values are similar to those previously measured in the prostate cancer cell line LNCaP (n = 19), where the intact peptide was found to comprise 15 ± 5% of all peptide present after 5 min and the 5- and 8-residue fragments accounted for 13 ± 7% and 40 ± 13% of all peptide, respectively.[22]

A time-averaged rate of degradation of intact VI-B in each cell line was calculated by assuming 100 pg of total protein in each cell.[38] The time-averaged rate of degradation in PANC-1, CFPAC-1, and HPAF-II cells was determined to have a median of 0.02 zmol pg^{-1} s^{-1} (Q_1 and Q_3 of 0.007 and 0.06 zmol pg^{-1} s^{-1}); 0.06 zmol pg^{-1} s^{-1} (Q_1 and Q_3 of 0.03 and 0.09 zmol pg^{-1} s^{-1}); and 0.1 zmol pg^{-1} s^{-1} (Q_1 and Q_3 of 0.04 and 0.5 zmol pg^{-1} s^{-1}), respectively. The difference in amount of peptide breakdown between cell lines was not statistically significant, with p-values of 0.1710 (PANC-1 vs CFPAC-1), 0.5735 (PANC-1 vs HPAF-II), and 0.9008 (CFPAC-1 vs HPAF-II). In each cell line, a plot of the time-averaged rate of degradation of intact VI-B as a function of initial substrate concentration revealed a direct linear correspondence between rate and substrate concentration (Figure S2, Supporting Information). These time-averaged rates of degradation did not statistically differ (p-values all greater than 0.07) from that previously reported for the degradation of peptide VI-B in LNCaP lysates, with a median rate of 0.02 zmol pg^{-1} s^{-1} (Q_1 and Q_3 of 0.007 zmol pg^{-1} s^{-1} and 0.05 zmol pg^{-1} s^{-1}).[22] The first-order relationship between degradation rate and substrate concentration suggested that the capacity of the endogenous peptidases was not saturated, even though substrate concentration in individual cells varied over 3 orders of magnitude. Similar observations have been previously reported.[39−41] This capacity for peptide metabolism may be the result of the need to rapidly recycle large quantities of damaged proteins produced in these rapidly growing tumor cells.

Measurement of PKB Activation in Single Tissue-Cultured Cells Derived from Pancreatic Adenocarcinomas. In addition to the two fragment peaks observed in single cells, phosphorylation of peptide VI-B was likewise seen in all three cell types. After peptide VI-B was incubated in PANC-1 cells for 5 min (Figure 1C), the median amount of phosphorylation was 65% (Q_1 = 48% and Q_3 = 71%). Assuming a total protein content of 100 pg per cell, the median time-averaged rate of phosphorylation was 0.01 zmol pg^{-1} s^{-1} (Q_1 and Q_3 of 0.007 and 0.06 zmol pg^{-1} s^{-1}).

When peptide VI-B was incubated for 5 min in CFPAC-1 cells (Figure 1C), the median amount of phosphorylation was 21% (Q_1 = 15% and Q_3 = 45%). The distribution of phosphorylated product appeared to be bimodal, with a cluster of 6 cells showing smaller amounts of phosphorylation (8−20%) and a cluster of 5 cells displaying larger amounts of phosphorylation (41−60%). Statistical analysis of a much larger population of cells will be required to evaluate whether or not the behavior of the CFPAC-1 cells is truly bimodal. Percent phosphorylation as a function of initial substrate concentration was plotted to determine if a bimodal variation of the amount of peptide injected into the cells would explain the varying distribution of phosphorylation. However, there appeared to be no correlation between initial substrate concentration and percent phosphorylation (data not shown). Assuming 100 pg of protein/cell, the median time-averaged rate of phosphorylation in single CFPAC-1 cells was 0.01 zmol pg^{-1} s^{-1} (Q_1 and Q_3 of 0.009 and 0.03 zmol pg^{-1} s^{-1}). The time-averaged rates between the two groups of cells likewise differed, with a median for the lower group of 0.01 zmol pg^{-1} s^{-1} (Q_1 and Q_3 of 0.008 and 0.08 zmol pg^{-1} s^{-1}) and a median for the higher group of 0.04 (Q_1 and Q_3 of 0.01 and 0.06 zmol pg^{-1} s^{-1}). Work by Cantley and others suggests that bimodal activation of the PKB signaling pathway may occur in some cell types and confer resistance to chemotherapy.[42−45]

In HPAF-II cells, the median amount of phosphorylation of VI-B after a 5 min incubation was 4% (Q_1 = 2% and Q_3 = 7%; Figure 1C) and the median time-averaged rate of phosphorylation was 0.005 zmol pg^{-1} s^{-1} (Q_1 and Q_3 of 0.002 and 0.01 zmol pg^{-1} s^{-1}). Single-cell analysis of substrate phosphorylation in intact, single PANC-1, CFPAC-1, and HPAF-II cells revealed a difference in the time-averaged rate of PKB activity among the three lines, indicating high, moderate, and low amounts of active PKB in the cells, respectively. A nonparametric Kruskal−Wallis statistical analysis of variance of these three populations demonstrated a statistically significant difference between the three populations (p-value of 4.4×10^{-4}). Previous work in the

dx.doi.org/10.1021/ac500616q | *Anal. Chem.* 2014, 86, 4573−4580

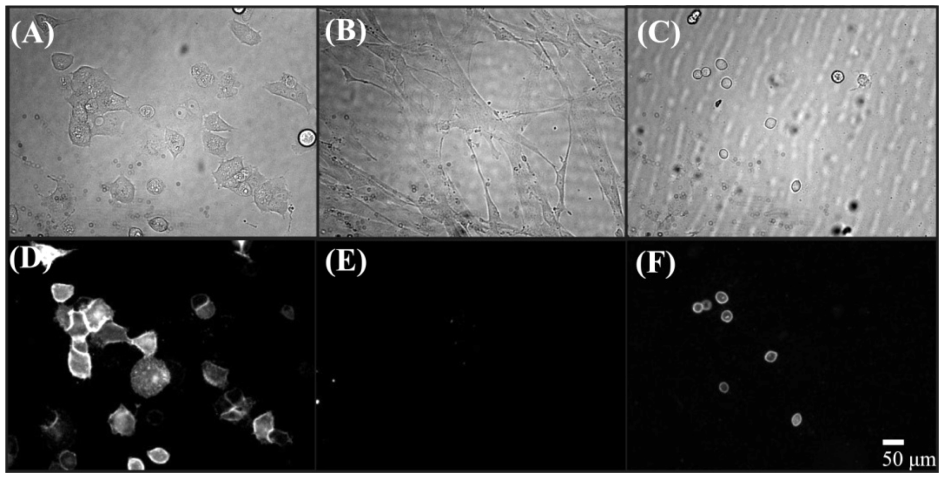

Figure 2. Brightfield (A–C) and fluorescence (D–F) images of cells cultured on polystyrene coverslips and stained with the AlexaFluor647 anti-EpCAM antibody. Shown are PANC-1 cells (A,D); WI-38 cells (B,E); and PDX tumor cells (C,F).

prostate cancer cell line LNCaP revealed a median phosphorylation percentage of 31% (Q_1 and Q_3 of 12% and 44%) and a median time-averaged phosphorylation rate of 0.01 zmol pg^{-1} s^{-1} (Q_1 and Q_3 of 0.004 and 0.03 zmol pg^{-1} s^{-1}), similar to the median of the CFPAC-1 cells.[22]

Inhibition of PKB Activity in Tissue-Cultured Cells. Wortmannin is an irreversible inhibitor of PI3-K at nanomolar levels, blocking the phosphorylation of phoshatidylinositol (4,5)-bisphosphate (PIP_2) to phosphatidylinositol (3,4,5)-trisphosphate (PIP_3).[46] PIP_3 recruits PKB to the plasma membrane which leads to PKB phosphorylation and activation. To determine whether phosphorylation of peptide VI-B was sensitive to wortmannin, PANC-1 (n = 11), CFPAC-1 (n = 11), and HPAF-II (n = 10) cells were incubated with 500 nM wortmannin prior to microinjection of peptide VI-B into single cells and subsequent electrophoresis. In all three cell lines, incubation with wortmannin eliminated the phosphorylation of the peptide in single cells (Figure 1C). In all cases, there was a statistical difference in the amount of VI-B phosphorylated in treated and untreated cells (p-value $<1 \times 10^{-4}$ for all three cell types). Inhibition of VI-B phosphorylation at these low wortmannin concentrations suggests that the peptide was predominantly acting as a substrate for PKB, as the wortmannin concentration used was an order of magnitude less than that reported for efficient inhibition of MLCK, the next kinase most susceptible to wortmannin.[46] Degradation of peptide VI-B was observed in all wortmannin-treated cells, and both the 8- and 5-residue fragments were observed in the majority of the wortmannin-treated cells (Figures 1B and S2, Supporting Information). A plot of the time-averaged rate of degradation of parent peptide VI-B as a function of initial substrate concentration (Figure S2, Supporting Information) revealed a linear correlation with a positive slope. Furthermore, there was no statistical difference between the time-averaged rate of peptide degradation in wortmannin-treated and untreated cells (p-values of 0.7705, 0.8810, and 0.9999 for PANC-1, CFPAC-1, and HPAF-II cells, respectively.)

Active PKB Determined by Western Blot Analysis in Cell Lysates Derived from Pancreatic Adenocarcinomas. Western blot analysis was performed to compare single cell results with the traditional bulk lysate measurements of PKB activity for the three cell types (Figure 1D). Total PKB was determined using an anti-PKB antibody sensitive to endogenous levels of PKB1, PKB2, and PKB3. Active PKB was determined using a monoclonal antibody against the phosphorylated serine at position 473. The same trend was observed as was seen in single cells, with PANC-1 cells showing the highest amount of phosphorylated PKB, CFPAC-1 cells a moderate amount, and HPAF-II cells the smallest amount. Although the averaged data from the single cell measurements matches that of the Western blots, single cell analysis revealed the cell-to-cell heterogeneity not available via the more traditional Western blot.

Wortmannin also decreased the amount of phosphorylated Ser473 in the cell lysates, as determined by Western blot (Figure 1D). The amount of pSer473 decreased in all three cell lines when wortmannin was present, though the total amount of PKB remained the same in treated and untreated samples.

Phosphorylation of Peptide VI-B over Time. To determine the effect of incubation time on peptide phosphorylation, peptide VI-B was microinjected into single tissue-cultured cells and incubated for 1, 3, 5, 10, or 30 min (Figure S3A–C, Supporting Information). In all cases, at least 10 cells were analyzed for each time point. For all three cell types, only a single HPAF-II cell showed phosphorylated product after a 1 min incubation. After a 3 min incubation, the CFPAC-1 cells displayed the highest percentage of phosphorylated product when compared to PANC-1 and HPAF-II cells. PANC-1 had the highest median amount of phosphorylation after a 5 min incubation, as described in the section Measurement of PKB Activation in Single Tissue-Cultured Cells Derived from Pancreatic Adenocarcinomas. This result held true at the 10 and 30 min time points as well. Table S1 (Supporting Information) summarizes the median data with the first and third quartiles for all 3 cells types at all incubation times. There is heterogeneity in the amount of phosphorylated product at nearly all time points sampled in all three cell types, although the median amount of phosphorylated product peaked at 5 min and decreased over time in the PANC-1 and CFPAC-1 cells and appeared to level off after 5 min in the HPAF-II cells.

The time-averaged rate of phosphorylation as a function of the initial substrate concentration for each cell type was plotted in order to identify whether the initial amount of substrate peptide loaded into each cell influenced the time-averaged phosphorylation rate (Figure S3D–F, Supporting Information). In all cell types at all 5 time points, a linear correlation was

dx.doi.org/10.1021/ac500616q | Anal. Chem. 2014, 86, 4573–4580

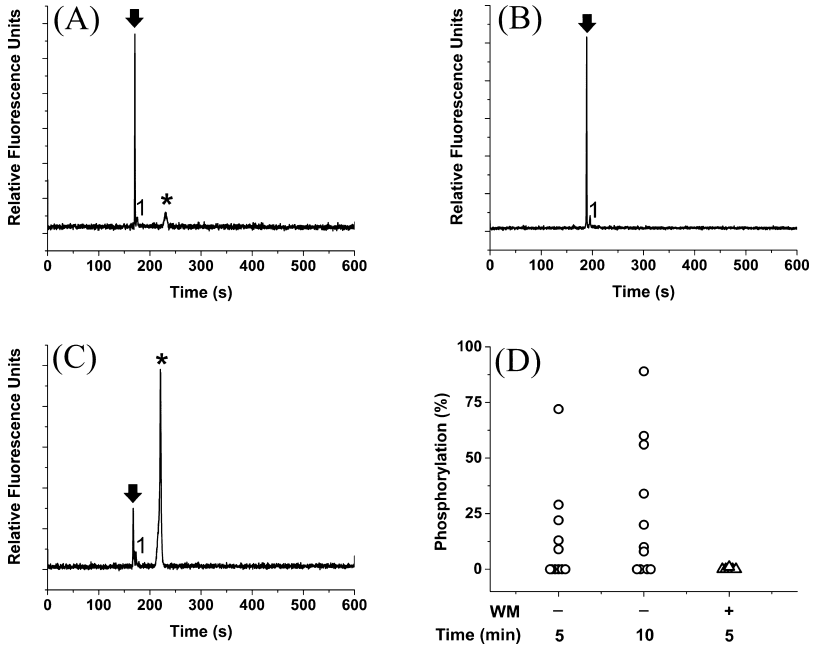

Figure 3. Electropherograms of single EpCAM$^+$ PDX tumor cells (A–C). Peptide VI-B was incubated in a single PDX tumor cell for 5 min without (A) and with (B) pretreatment with wortmannin. Peptide VI-B was incubated in a single PDX tumor cell for 10 min without treatment with wortmannin (C). The solid arrow indicates intact parent peptide, and the asterisk indicates phosphorylated peptide. Peak 1 corresponds to the 8-residue fragment peptide. (D) Percent of phosphorylated substrate in single, EpCAM$^+$ PDX tumor cells after different incubation times of peptide VI-B in the cells. WM stands for wortmannin.

(A)

	Cleavage Locations			
Cell Type	A-F	F-MeAla	Slope (zmol μM^{-1} s^{-1})	R^2
LNCaP*	Yes	Yes	2.0	0.99
PANC-1	Yes	Yes	9.5	0.49
CFPAC-1	Yes	Yes	15.3	0.56
HPAF-II	Yes	Yes	2.8	0.42
Xenograft	No	Yes	0.26	0.11

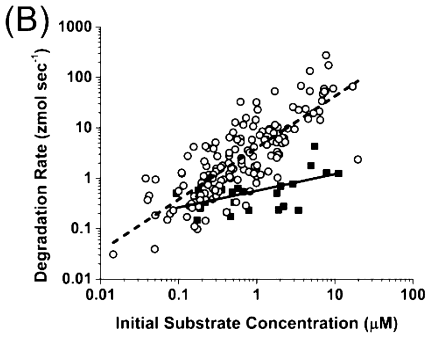

Figure 4. Degradation differences between tissue-cultured and PDX tumor cells. (A) Cleavage locations identified for each cell type tested. The prostate cancer line LNCaP* data is from Proctor et al.[22] The slope is defined as the change in the average degradation rate with respect to the initial substrate concentration. R^2 is the correlation coefficient for the fit of the straight line. (B) Degradation rate of peptide VI-B incubated in single pancreatic cancer tissue-cultured cells (open circles) or PDX tumor cells (closed squares) as a function of initial substrate concentration. The dashed line is the linear fit (R^2 = 0.3) of the tissue-cultured data, and the solid line is the linear fit (R^2 = 0.1) of the PDX tumor cell data.

observed, showing that as the initial substrate concentration increased so did the time-averaged rate. This correlation was independent of incubation time, as the same trend was observed for all time points in all three cell types.

Measurement of PKB Activation in Single Cells Derived from PDX Tumors. PDX tumor cells were readily distinguished from nontumor cells by the presence of epithelial cell adhesion molecule (EpCAM, also known as CD326) upon immunohistochemical staining (Figure 2C,F). In these experiments, PANC-1 cells (EpCAM$^+$) and WI-38 fibroblast cells (EpCAM$^-$) served as positive and negative staining controls, respectively, for these experiments (Figure 2A,B,D,E). PKB activation was measured in single tumor cells by staining the PDX tumor sample with anti-EpCAM antibody and then microinjecting peptide VI-B into the EpCAM$^+$ cells. Cells were incubated at 37 °C for 5 or 10 min and their contents separated by electrophoresis. Up to 3 peaks were observed in each single-cell electropherogram: the intact parent peptide; phosphorylated substrate; and the 8-residue fragment peptide (Figure 3). When incubated for 5 min, phosphorylation of peptide VI-B ranged from 0% to 72% of the undegraded peptide (n = 11). After a 10 min incubation, phosphorylation increased to 0–89% of total intact peptide (n = 11). The range of peptide phosphorylation, or PKB activation, in the PDX tumor cells was substantially broader than that for the cultured cell lines suggesting that the signaling pathways in PDX tumors were more heterogeneous than cultured cell lines. These results are consistent with the tumor heterogeneity observed during single-cell sequencing,[18] demonstrating the value of single-cell characterization in understanding tumor cell biology.

Inhibition of PKB Activity in Single Cells Derived from PDX Tumors. Cells were pretreated with wortmannin (500

dx.doi.org/10.1021/ac500616q | Anal. Chem. 2014, 86, 4573–4580

nM), stained with EpCAM, and then microinjected with peptide VI-B. After a 5 min incubation, 5 of 6 cells displayed two peaks on the electropherograms, which corresponded to intact parent peptide and the 8-residue fragment (Figure 3B,D). Phosphorylated peptide (1% of total intact peptide) was present in only a single cell. These data suggest that PKB was primarily responsible for phosphorylation of the substrate. When the mean phosphorylation observed in wortmannin-treated cells was compared to that seen in untreated cells at both the 5 and 10 min time points, a statistical difference in phosphorylation was observed (p-values of 0.0015 and 1×10^{-4}, respectively).

Degradation of Peptide VI-B in Single Cells Derived from PDX Tumors. In addition to the intact parent peptide and its phosphorylated counterpart, the 8-residue fragment peptide was also detected in the PDX tumor cells (Figures 3 and 4). However, it was present in much lower amounts than in the tissue-cultured lines previously tested, with a median of 11% of all peptide present (Q_1 and Q_3 of 7% and 12%). When compared against the standard tissue-cultured cells, this value was found to be significantly lower than in any of the three cell types analyzed (p-value of $<10^{-4}$ in all three cases.) The 5-residue fragment was not observed in any of the PDX tumor cells examined (n = 28), though it was prevalent in tissue-cultured cells. Figure 4A details the degradation pattern between tissue-cultured and PDX tumor cells.

For the PDX tumor cells, the average rate of peptide degradation depended on the initial substrate concentration (Figure 4B). When fit to a line, the slope was 0.26 zmol μM^{-1} s^{-1}, an order of magnitude less than that seen for the tissue-cultured cells in this work and in prior work using other tissue-cultured cells,[22] suggesting that the peptidases responsible for degradation of peptide VI-B are substantially less active in the PDX tumor cells compared to that in tissue-cultured cells. Analysis of covariance of the two regression lines generated an F-statistical value of 7.598 (yielding a p-value $<10^{-4}$) indicating that there was a statistical difference in the two regression lines.

CONCLUSIONS

A PKB substrate peptide was utilized as a dual reporter to simultaneously measure peptidase and kinase activity in single, intact pancreatic cancer cells. The reporter was degraded into two fragment peptides (a 5-mer and an 8-mer) in all three tissue-cultured cell types analyzed, similar to that observed in previous studies using prostate cancer cells.[22] Reporter degradation in single PDX tumor cells differed from that of the tissue-cultured cells in both the location of cleavage and the time-averaged rate of degradation. Although two cleavage sites were identified in tissue-cultured cells, only one (the 8-mer) was observed in the PDX tumor cells. A search of the peptidase database MEROPS[47] reveals that, of the common cytosolic peptidases, dipeptidyl peptidase II preferentially cleaves after an alanine residue, which would yield the 5-mer observed in these studies. Thus, it is possible that the tissue-cultured cells overexpress this particular cytosolic peptidase compared to the primary cells. This may be an adaptation of the tissue-cultured cell-lines to prolonged culture in an *in vitro* setting. In addition, the time-averaged rate of degradation in PDX tumor cells was an order of magnitude less than that seen in tissue-cultured cells, demonstrating that peptidases are less active or more tightly controlled in the PDX cells than the tissue-cultured lines which is likely a second adaptation to prolonged *in vitro* culture.

PKB activity was also assessed in single cells by comparing the amount of phosphorylated product to the amount of substrate loaded into each cell. High PKB activity in pancreatic cancer tumors is associated with resistance to apoptosis, higher rates of metastasis and mutations, and increased proliferation and uninhibited growth.[48] The PANC-1 tissue-cultured cells displayed the highest median amount of PKB activity of the three cell lines examined, implying that they are more adapted for survival in stressful environments and are likely to show increased rates of proliferation and resistance to stress compared to other cell types. Although a much larger population of CFPAC-1 cells would need to be analyzed to identify whether or not the PKB signaling is truly bimodal, our results suggest this might be a possibility. If high and low states of PKB activity do exist within this population, it would provide these cells with a means to survive chemotherapeutic insults, with the population shifting to one extreme or the other in response to drug treatment.

The PKB activity measured in the PDX cells varied more than that seen in the tissue-cultured cells, with many cells showing no PKB activity and others demonstrating very high levels of substrate phosphorylation. This suggests that the individual cells in the animal might be adapted to the different environmental conditions within the tumor whereas the tissue-cultured cells are expected to experience significantly less environmental variability. For example, a low pH and anoxic tumor region might require greater PKB activity to survive the resulting stresses compared to a well-vascularized, lower-stress region of a tumor. The tumor heterogeneity would ensure tumor survival under the varying conditions found *in vivo*.

As this technology matures to become higher throughput, single-cell CE may be of value in monitoring PKB activity levels in single cells from patients diagnosed with PDA. Previous studies have shown that inhibition of the PI3-K/PKB pathway sensitizes pancreatic cancer cells to chemotherapy.[48,49] Thus, a better understanding of whether the PI3-K/PKB pathway is active in a patient's tumor as well as knowledge of the diversity in single-cell signaling would be a valuable guide to tailoring chemotherapeutics. Single-cell CE can be used to determine the effectiveness PI3-K/PKB pathway inhibition within a cell population and whether a subset of cells has become resistant to PI3-K/PKB pathway-targeted therapeutics. Tracking the evolution of PI3-K/PKB pathway signaling in a tumor in response to therapy may enable more tailored therapeutic strategies than currently available.

ASSOCIATED CONTENT

Supporting Information

Additional information as noted in text. This material is available free of charge via the Internet at http://pubs.acs.org.

AUTHOR INFORMATION

Corresponding Author

*E-mail: nlallbri@unc.edu. Fax: 919-962-2388.

Notes

The authors declare no competing financial interest.

ACKNOWLEDGMENTS

The authors would like to thank Jadwiga K. Smyla for preparation of the PDX tumor single cells. This work was supported by the NIH (CA139599 and CA140173).

REFERENCES

(1) Agbunag, C.; Bar-Sagi, D. *Cancer Res.* **2004**, *64*, 5659−5663.
(2) Asano, T.; Yao, Y.; Zhu, J.; Li, D.; Abbruzzese, J. L.; Reddy, S. A. G. *Oncogene* **2004**, *23*, 8571−8589.
(3) Bardessy, N.; DePinho, R. A. *Nat. Rev. Cancer* **2002**, *2*, 897−909.
(4) Donahue, T. R.; Tran, L. M.; Hill, R.; Li, Y.; Kovochich, A.; Calvopina, J. H.; Patel, S. G.; Wu, N.; Hindoyan, A.; Farrell, J. J.; Li, X.; Dawson, D. W.; Wu, H. *Clin. Cancer Res.* **2012**, *18*, 1352−1363.
(5) American Cancer Society. *Cancer Facts and Figures 2013*; American Cancer Society: Atlanta, 2013.
(6) Hezel, A. F.; Kimmelman, A. C.; Stanger, B. Z.; Bardeesy, N.; DePinho, R. A. *Genes Dev.* **2006**, *20*, 1218−1249.
(7) Jones, S.; Zhang, X.; Parsons, D. W.; Lin, J. C.; Learly, R. J.; Angenendt, P.; Mankoo, P.; Carter, H.; Kamiyama, H.; Jimeno, A.; Hong, S.; Fu, B.; Lin, M.; Calhoun, E. S.; Kamiyama, M.; Walter, K.; Nikolskaya, T.; Nikolsky, Y.; Hartigan, J.; Smith, D. R.; Hidalgo, M.; Leach, S. D.; Klein, A. P.; Jaffee, E. M.; Goggins, M.; Maitra, A.; Iacobuzio-Donahue, C.; Eshleman, J. R.; Kern, S. E.; Hruban, R. H.; Karchin, R.; Papadopoulos, N.; Parmigiani, G.; Vogelstein, B.; Velculescu, V. E.; Kinzler, K. W. *Science* **2008**, *321*, 1801−1806.
(8) Arlt, A.; Müerköster, S. S.; Schäfer, H. *Cancer Lett.* **2013**, *332*, 346−358.
(9) Hidalgo, M. *N. Engl. J. Med.* **2010**, *362*, 1605−1617.
(10) Brazil, D. P.; Park, J.; Hemmings, B. A. *Cell* **2002**, *111*, 293−303.
(11) Brazil, D. P.; Hemmings, B. A. *Trends Biochem. Sci.* **2001**, *26*, 657−664.
(12) Edling, C. E.; Selvaggi, F.; Buus, R.; Maffucci, T.; Di Sebastiano, P.; Friess, H.; Innocenti, P.; Kocher, H. M.; Falasca, M. *Clin. Cancer Res.* **2010**, *16*, 4928−4937.
(13) Parsons, C. M.; Muilenburg, D.; Bowles, T. L.; Mirudachalam, S.; Bold, R. J. *Anticancer Res.* **2010**, *30*, 3279−3290.
(14) Schlieman, M. G.; Fahy, B. N.; Ramsamooj, R.; Beckett, L.; Bold, R. J. *Br. J. Cancer* **2003**, *89*, 2110−2115.
(15) Yamamoto, S.; Tomita, Y.; Hoshida, Y.; Morooka, T.; Nagano, H.; Dono, K.; Umeshita, K.; Sakon, M.; Ishikawa, O. *Clin. Cancer Res.* **2004**, *10*, 2846−2850.
(16) Zavoral, M.; Minarikova, P.; Zavada, F.; Salek, C.; Minarik, M. *World J. Gastroenterol.* **2001**, *17*, 2897−2908.
(17) Samuel, N.; Hudson, T. J. *Nat. Rev. Gastroenterol. Hepatol.* **2012**, *9*, 77−87.
(18) Marusyk, A.; Almendro, V.; Polyak, K. *Nat. Rev. Cancer* **2012**, *12*, 323−334.
(19) Fidler, I. J. *Cancer Res.* **1978**, *38*, 2651−2660.
(20) Heppner, G. H. *Cancer Res.* **1984**, *44*, 2259−2265.
(21) Dovichi, N. J. In *Chemical Cytometry: Ultrasensitive Analysis of Single Cells*; Lu, C., Ed.; Wiley-VCH: Weinheim, 2010; pp 1−19.
(22) Proctor, A.; Wang, Q.; Lawrence, D. S.; Allbritton, N. L. *Anal. Chem.* **2012**, *84*, 7195−7202.
(23) Garber, K. *J. Natl. Cancer Inst.* **2009**, *101*, 6.
(24) Moro, M.; Berolinia, G.; Tortoreto, M.; Pastorino, U.; Sozzi, G.; Roz, L. *J. Biomed. Biotechnol.* **2012**, *2012*, 1−11.
(25) Hidalgo, M.; Bruckheimer, E.; Rajeshkumar, N. V.; Garrido-Laguna, I.; De Oliveira, E.; Rubio-Viqueira, B.; Strawn, S.; Wick, M. J.; Martell, J.; Sidransky, D. *Mol. Cancer Ther.* **2011**, *10*, 1311−1316.
(26) Decaudin, D. *Anti-Cancer Drugs* **2011**, *22*, 827−841.
(27) Neel, N. F.; Stratford, J. K.; Shinde, V.; Ecsedy, J. A.; Martin, T. D.; Der, C. J.; Yeh, J. J. *Mol. Cancer Ther.* **2014**, *13*, 122−133.
(28) Hahn, S. A.; Seymour, A. B.; Shamsul Hoque, A. T. M.; Schutte, M.; da Costa, L. T.; Redston, M. S.; Caldas, C.; Weinstein, C. L.; Fischer, A.; Yeo, C. J.; Hruban, R. H.; Kern, S. E. *Cancer Res.* **1995**, *55*, 4670−4675.
(29) Metzgar, R. S.; Gaillard, M. T.; Levine, S. J.; Tuck, F. L.; Bossen, E. H.; Borowitz, M. J. *Cancer Res.* **1982**, *42*, 601−608.
(30) Schoumacher, R. A.; Ram, J.; Iannuzzi, M. C.; Bradbury, N. A.; Wallace, R. W.; Tom Hon, C.; Kelly, D. R.; Schmid, S. M.; Gelder, F. B.; Rado, T. A.; Frizzell, R. A. *Proc. Natl. Acad. Sci. U.S.A.* **1990**, *87*, 4012−4016.
(31) Lieber, M.; Mazzetta, J.; Nelson-Rees, W.; Kaplan, M.; Todaro, G. *Int. J. Cancer* **1975**, *15*, 741−747.
(32) Hayflick, L.; Moorhead, P. S. *Exp. Cell Res.* **1961**, *25*, 585−621.
(33) Bang, D.; Wilson, W.; Ryan, M.; Yeh, J. J.; Baldwin, A. S. *Cancer Discovery* **2013**, *3*, 690−703.
(34) Wang, Y.; Balowski, J.; Phillips, C.; Phillips, R.; Sims, C. E.; Allbritton, N. L. *Lab Chip* **2011**, *11*, 3089−3097.
(35) Sims, C. E.; Meredith, G. D.; Krasieva, T. B.; Berns, M. W.; Tromberg, B. J.; Allbritton, N. L. *Anal. Chem.* **1998**, *70*, 4570−4577.
(36) Kottegoda, S.; Aoto, P. C.; Sims, C. E.; Allbritton, N. L. *Anal. Chem.* **2008**, *80*, 5358−5366.
(37) Meredith, G. D.; Sims, C. E.; Soughayer, J. S.; Allbritton, N. L. *Nat. Biotechnol.* **2000**, *18*, 309−312.
(38) Schmid, A.; Kortmann, H.; Dittrich, P. S.; Blank, L. M. *Curr. Opin. Biotechol.* **2010**, *21*, 12−20.
(39) Kovarik, M. L.; Shah, P. K.; Armistead, P. M.; Allbritton, N. L. *Anal. Chem.* **2013**, *85*, 4991−4997.
(40) Brown, R. B.; Hewel, J. A.; Emili, A.; Audet, J. *Cytometry, Part A* **2010**, *77A*, 347−355.
(41) Reits, E.; Griekspoor, A.; Neijssen, J.; Groothuis, T.; Jalink, K.; van Veelen, P.; Janssen, H.; Calafat, J.; Drijfhout, J. W.; Neefjes, J. *Immunity* **2003**, *18*, 97−108.
(42) Yuan, T. L.; Wulf, G.; Burga, L.; Cantley, L. C. *Curr. Biol.* **2011**, *21*, 173−183.
(43) Perez, O. D.; Kinoshita, S.; Hitoshi, Y.; Payan, D. G.; Kitamura, T.; Nolan, G. P.; Lorens, J. B. *Immunity* **2002**, *16*, 51−65.
(44) Perez, O. D.; Nolan, G. N. *Nat. Biotechnol.* **2002**, *20*, 155−162.
(45) Heffner, G. C.; Clutter, M. R.; Nolan, G. P.; Weissman, I. L. *Stem Cells* **2011**, *29*, 1774−1782.
(46) Bain, J.; Plater, L.; Elliott, M.; Shpiro, N.; Hastie, C. J.; McLauchlan, H.; Klevernic, I.; Arthur, J. S. C.; Alessi, D. R.; Cohen, P. *Biochem. J.* **2007**, *408*, 297−315.
(47) Rawlings, N. D.; Barrett, A. J.; Bateman, A. *Nucleic Acids Res.* **2012**, *40*, D343−D350. URL: merops.sanger.ac.uk/index.shtml.
(48) Ottenhof, N. A.; de Wilde, R. F.; Maitra, A.; Hruban, R. H.; Offerhaus, G. J. A. *Pathol. Res. Int.* **2011**, No. 620601.
(49) Roy, S. K.; Srivastava, R. K.; Shankar, S. *J. Mol. Signaling* **2010**, *5*, 10.